

The α/β -hydrolase domain 6 inhibitor WWL70 decreases endotoxin-induced lung inflammation in mice, potential contribution of 2-arachidonoylglycerol, and lysoglycerophospholipids

Pauline Botteman, Adrien Paquot, Hafsa Ameraoui, Mireille Alhouayek, and Giulio G. Muccioli¹

Bioanalysis and Pharmacology of Bioactive Lipids Research Group, Louvain Drug Research Institute, Université Catholique de Louvain (UCLouvain), Brussels, Belgium

ABSTRACT: Lung inflammation plays a crucial role in the pathogenesis of many respiratory diseases that are in need of new therapeutic strategies. Previously, we showed that inhibition of α/β -hydrolase domain 6 (ABHD6) decreased macrophage activation and exerted anti-inflammatory effects. Therefore, we thought to assess the effects of ABHD6 inhibition in a mouse model of acute lung injury (ALI) induced by intratracheal administration of lipopolysaccharides. ABHD6 inhibition with *N*-methyl-*N*-[3-(4-pyridinyl)phenyl]methyl-carbamic acid 4'-(aminocarbonyl)(1,1'-biphenyl)-4-yl ester (WWL70) decreases most of the hallmarks of ALI, including neutrophil infiltration, cytokine secretion, and protein extravasation. mRNA expression of proinflammatory markers in the cells recovered in the bronchoalveolar lavage was also decreased. Interestingly, ABHD6 inhibition was more efficient than monoacylglycerol lipase inhibition by 4-nitrophenyl-4-[dibenzo(d)(14)dioxol-5-yl(hydroxy)methyl]piperidine-1-carboxylate. We also studied ABHD6 inhibition on primary alveolar macrophages and neutrophils to explore their potential implication in the effects of ABHD6 inhibition *in vivo*. Moreover, we quantified by high-performance liquid chromatography–mass spectrometry the levels of reported substrates of ABHD6 [*i.e.*, 2-arachidonoylglycerol (2-AG) and lysophospholipids]. The potential implication of these lipid mediators in the effects of WWL70 was further investigated on primary alveolar macrophages. Taken together, these data support ABHD6 inhibition as an interesting anti-inflammatory strategy in acute lung inflammation and assess the possible contribution of 2-AG and lysophospholipids in the observed effects.—Botteman, P., Paquot, A., Ameraoui, H., Alhouayek, M., Muccioli, G. G. The α/β -hydrolase domain 6 inhibitor WWL70 decreases endotoxin-induced lung inflammation in mice, potential contribution of 2-arachidonoylglycerol, and lysoglycerophospholipids. *FASEB J.* 33, 7635–7646 (2019). www.fasebj.org

KEY WORDS: serine hydrolase • bioactive lipid • MAGL • prostaglandin • PGE₂

Acute lung injury (ALI) and its more severe manifestation, acute respiratory distress syndrome, are often seen as part of a systemic inflammatory process. The inflammatory response occurring in the lung is characterized, among others, by an increase in endothelial and epithelial permeability leading to extravasation of protein-rich fluid and interstitial edema with bilateral pulmonary infiltrates containing neutrophils and an array of pro- and anti-inflammatory

cytokines (1). Over the years, the mortality rates associated with ALI have decreased; however, ALI still affects long-term quality of life of patients (2, 3). Moreover, depending on the underlying disorder, mortality remains high in some cases, such as sepsis and multiorgan failure (30–40%) (4). Currently, very few pharmacological treatments are available for ALI. Several strategies have been investigated, such as targeting individual proinflammatory cytokines or the

ABBREVIATIONS: 2-AG, 2-arachidonoylglycerol; ABHD6, α/β -hydrolase domain 6; ALI, acute lung injury; BAL, bronchoalveolar lavage; HPGDS, hematopoietic prostaglandin D synthase; HTAB, hexadecyltrimethylammonium bromide; HPLC, high-performance liquid chromatography; JZL184, 4-nitrophenyl-4-[dibenzo(d)(14)dioxol-5-yl(hydroxy)methyl]piperidine-1-carboxylate; KC, keratinocyte chemokine; KT182, 4-[3'-(hydroxymethyl)(1,1'-biphenyl)-4-yl]-1H-1,2,3-triazol-1-yl(2-phenyl-1-piperidinyl)-methanone; LPS, lipopolysaccharide; LPS-veh, untreated LPS; LTA, lipoteichoic acid; lysoPC, lysophosphatidylcholine; lysoPE, lysophosphatidylethanolamine; lysoPG, lysophosphatidylglycerol; lysoPI, lysophosphatidylinositol; lysoPS, lysophosphatidylserine; MAGL, monoacylglycerol lipase; MCP1, monocyte chemoattractant protein 1; MIP2 α , macrophage inflammatory protein 2 α ; mPGES, microsomal prostaglandin E synthase; MPO, myeloperoxidase; MS, mass spectrometry; PGE₂, prostaglandin E₂; q-PCR, quantitative PCR; RPL19, ribosomal protein L19; WWL70, *N*-methyl-*N*-[3-(4-pyridinyl)phenyl]methyl-carbamic acid 4'-(aminocarbonyl)(1,1'-biphenyl)-4-yl ester

¹ Correspondence: Bioanalysis and Pharmacology of Bioactive Lipids Research Group, Louvain Drug Research Institute, Université Catholique de Louvain (UCLouvain), Av. E. Mounier, 72 (B1.72.01), 1200 Brussels, Belgium. E-mail: giulio.muccioli@uclouvain.be

doi: 10.1096/fj.201802259R

This article includes supplemental data. Please visit <http://www.fasebj.org> to obtain this information.

NF- κ B pathway among others. However, only corticosteroids and statins have shown some beneficial effects in ALI treatment (5). Therefore, there is a clear need for therapeutic strategies for ALI.

A common experimental model of ALI is the airway instillation of endotoxins, typically bacterial LPS, in mice (1, 6). In this model, as in ALI patients, macrophages are key regulators of lung inflammation (1). At steady state, alveolar macrophages are important for maintaining homeostasis and tolerance toward nonharmful antigens penetrating the lungs (7–9). Upon activation, they will orchestrate the immune response allowing to clear the antigens and to restore homeostasis *via* the control of the resolution process (7). Failure in these events can lead to unbalanced or chronic inflammation (10). Along with alveolar macrophages, neutrophils are thought to play a major role in the early event of the development of ALI, and decreasing their recruitment is therefore crucial (4). Indeed, neutrophils are the first immune cells recruited to the site of injury (11). They have an important antimicrobial role, but an uncontrolled activation can induce tissue damages. Controlling their recruitment, their activation, or the release of their antimicrobial molecules could therefore have beneficial effects on the pathology.

Modulating bioactive lipid levels is emerging as an interesting strategy to tackle inflammation. In this context, the endocannabinoid 2-arachidonoylglycerol (2-AG) is clearly a prime example (12). Indeed, this endocannabinoid is involved in the regulation of several physiologic or pathophysiologic processes, including inflammation, through the activation of the cannabinoid receptors. 2-AG is synthesized from membrane phospholipids and inactivated by serine hydrolases with a predominant role for monoacylglycerol lipase (MAGL) (12, 13). Although little is known on the effect of 2-AG in the lungs, a report described that MAGL inhibition reduces lung inflammation in a model of ALI obtained by intranasal administration of LPS (14). Besides MAGL, we and others have shown that 2-AG levels can be modulated in cells (and notably macrophages) and tissues by the serine hydrolase α/β -hydrolase domain 6 (ABHD6) (15–18). We have also shown that inhibition of ABHD6 results in decreased LPS-induced macrophage activation and inflammation (18). Interestingly, evidence supports the ability of ABHD6 to hydrolyze, besides monoacylglycerols, several lysoglycerophospholipid families (19, 20).

Because macrophages are key players in acute lung inflammation, and because we previously showed that ABHD6 inhibition decreases macrophage activation, we thought to investigate the effect of ABHD6 inhibition on LPS-induced lung inflammation. To gain some mechanistic insights, our results prompted us to assess, using primary alveolar macrophages, how the substrates of ABHD6 would affect LPS-induced macrophage activation. We also studied a potential involvement of neutrophils in the effects of the ABHD6 inhibitor.

MATERIALS AND METHODS

Animals

Male CD1 mice (Janvier Labs, Le Genest-Saint-Isle, France) 7–8 wk old, were used in all experiments. They were housed in

filter-top cages under conditions of controlled temperature (20–22°C) and artificial light (12-h light/dark) and supplied with drinking water and food *ad libitum*. All animal procedures were performed under ketamine and xylazine anesthesia, and all efforts were made to minimize suffering. All animal experiments were performed in accordance with the guidelines of the local ethics committee and in accordance with European Directive 2010/63/EU, which was transformed into the Belgian law of May 29, 2013, regarding the protection of laboratory animals. The local ethics committee of the Université Catholique de Louvain reviewed and approved the experimental protocols (2017/UCL/MD/024, laboratory agreement LA1230635).

Drugs

LPS (*Escherichia coli*, O55:B5), hexadecyltrimethylammonium bromide (HTAB), *o*-dianisidine, and the ABHD6 inhibitor 4-[3'-(hydroxymethyl)(1,1'-biphenyl)-4-yl]-1H-1,2,3-triazol-1-yl(2-phenyl-1-piperidinyl)-methanone (KT182) were obtained from MilliporeSigma (Merck, Darmstadt, Germany). The ABHD6 inhibitor *N*-methyl-*N*-[3-(4-pyridinyl)phenyl]methylcarbamate 4'-(aminocarbonyl)(1,1'-biphenyl)-4-yl ester (WWL70), the MAGL inhibitor 4-nitrophenyl-4-[dibenzo(d)(14)dioxol-5-yl(hydroxy)methyl]piperidine-1-carboxylate (JZL184), 2-AG, and deuterated 2-AG (d_5 -2AG) were from Cayman Chemicals (Ann Arbor, MI, USA) and purchased from Sanbio (Uden, The Netherlands). Lysophospholipids [lysophosphatidylethanolamine (lysoPE), lysophosphatidylglycerol (lysoPG), lysophosphatidylinositol (lysoPI), lysophosphatidylserine (lysoPS), and lysophosphatidylcholine (lysoPC)] were purchased from Avanti Polar Lipids (Alabaster, AL, USA). Lipoteichoic acid (LTA) was from InvivoGen (San Diego, CA, USA).

ALI model

The mice were anesthetized with an intraperitoneal injection of ketamine (100 mg/kg) and xylazine (10 mg/kg) before intratracheal instillation (30 μ l/mouse) of LPS or vehicle (sterile 0.9% saline) followed by 0.1 ml of air. We used LPS at a concentration of 200 μ g/ml (21, 22). After intratracheal treatment, mice were kept in an upright position for 5 min to allow sufficient spreading of the fluid throughout the lungs. After LPS exposure (24 h), mice were anesthetized and euthanized by cervical dislocation. The bronchoalveolar lavage (BAL) fluid and the lungs were recovered for further analyses.

For drug treatment, the MAGL inhibitor JZL184 (16 mg/kg) and the ABHD6 inhibitor WWL70 (20 mg/kg) were administered intraperitoneally 1 h before LPS instillation. Control mice and untreated mice receiving LPS received an intraperitoneal injection of the vehicle [saline, ethanol, and Tween 80 (18:1:1, v/v/v)]. For the therapeutic intervention study, WWL70 (20 mg/kg) was administered 1 h after the induction of lung inflammation. The doses and the treatment were based on previously published studies (14, 18, and 23).

BAL

BAL was performed after euthanizing the mice by cervical dislocation under anesthesia. PBS (1 ml) supplemented with EDTA (0.5 mM) and protease inhibitors were injected into the trachea through a cannula. All the BAL fluid was removed from the lungs afterwards. The volume of recovered BAL fluid was recorded. Five lavages were performed in total. The samples from the first lavage were centrifuged at 250 *g* for 5 min. The supernatants were collected and stored at –80°C to measure protein concentration and cytokine secretion. The cell pellets from all 5 lavages were

resuspended in PBS-EDTA buffer. An aliquot of the cell suspension was used for differential cell counts and the remaining was centrifuged at 250 g for 5 min. The resulting cell pellet was snap frozen in liquid nitrogen for further assessment. After the BAL procedure, the lungs were resected and snap frozen in liquid nitrogen.

Total and differential leukocyte counts

Total leukocytes were counted using a cell suspension in Turk’s solution. The differential cell counts were obtained by cytocentrifugation and coloration with Diff-Quik (Medion Diagnostics, Miami, FL, USA). Following slide digitalization, macrophages, neutrophils, and lymphocytes were counted based on cell morphology, at a ×40 magnification, by counting 300 cells per slide and recording cell numbers of each type in a blind fashion. The percentages of each cell type were then calculated. The numbers of cell components were determined by multiplying the total cell number with the percentages of each cell type.

Protein quantification in the BAL

Total protein concentration was determined using the DC Protein Assay (Bio-Rad, Hercules, CA, USA) following the manufacturer’s instructions and using 5 µl of BAL fluid supernatant. Absorbance was read at 750 nm, and a calibration curve made with bovine serum albumin was used.

Cytokine quantification by ELISA

Levels of proinflammatory cytokines (IL-6 and TNF-α) in the BAL fluid supernatant were determined by a sandwich-type ELISA technique using the Ready-Set-Go! Kit (Thermo Fisher Scientific, Waltham, MA, USA) following the manufacturer’s instructions (24).

Myeloperoxidase assay

The tissue-associated myeloperoxidase (MPO) assay was performed as previously described by Alhouayek *et al.* (25) to quantify the degree of neutrophil infiltration in the lungs, which correlates with the severity of lung injury (11). In brief, the left lung was snap frozen in liquid nitrogen at the time of killing and stored for later assessment. For determination of MPO activity, tissue was homogenized in HTAB buffer [0.5% HTAB in 50 mM potassium phosphate buffer (pH 6)]. The volume of buffer was corrected to lung weight. The homogenate was centrifuged at 20,000 g for 20 min at 4°C and the supernatant was recovered. The supernatant (8 µl) was then added to 96-well plates together with 200 µl of a solution of 0.167 mg/ml o-dianisidine and 5 parts per million hydrogen peroxide in 50 mM potassium phosphate buffer at pH 6. Samples were analyzed in duplicate. MPO activity in the supernatant was measured at 460 nm and normalized for protein concentration.

RNA extraction and real-time quantitative PCR

Total RNA was extracted using the TriPure reagent (Roche, Basel, Switzerland) according to the manufacturer’s instructions. cDNA was synthesized using a Reverse Transcription Kit (RT GoScript mix; Promega, Madison, WI, USA). Quantitative PCR (qPCR) was performed with a StepOnePlus instrument and software (Thermo Fisher Scientific). Products were analyzed by performing a melting curve at the end of the PCR (26). Data are normalized to the 60S ribosomal protein L19 (RPL19) mRNA expression. Primer sequences for quantitative PCR are listed in Table 1, along

TABLE 1. Primer sequences for murine samples

Gene/product	Primer (5'–3')		Accession no.	Product length (bp)
	Forward	Reverse		
<i>Rpl19/RPL19</i>	TGACCTGGATGAGAAGGATGAG	CTGTCATACATATGGCGGTCAATC	NM_001159483.1 and NM_009078.2	88
<i>Tnf/TNF-α</i>	CTACTGAACCTCGGGGTGATC	TGAGTGTGAGGTCGTGGC	NM_013693.3 and NM_001278601.1	94
<i>Il6/IL-6</i>	ACAAAGTCGGAGGCTTAATTACACAT	TTGCCATTGCACAACTCTTTTC	NM_001314054.1 and NM_031168.2	72
<i>Cxcl2/MIP2α</i>	CAGACAGAAATCATAGCCATC	CCTTCCAGGTCACTTAGCC	NM_009140.2	124
<i>Cxcl1/KC</i>	GGCTGGGATTCACCTCAAG	GAGTGTGGCTATGACTTCGG	NM_008176.3	88
<i>Ccl2/MCP1</i>	GTCCCAAGAAAGCTGTAGTTTTC	ATGTATGTCTGGACCATTC	NM_011333.3	85
<i>Mgll/MAGL</i>	ATGTCCTGATTTACCTCTGGT	TCAACTCCGACTTGTCCGAGACA	NM_001166251.1 and NM_011844.4 and NM_001166249.1	152
<i>Abhd6/ABHD6</i>	CTGTCCATAGTGGGCAAGT	TCAGATGGGTAGTAAGCGGC	NM_001331065.1 and NM_001331064.1 and NM_025341.4	137
<i>Piges/mPGES1</i>	ATGAGGCTGGGGAAGG	GCCGAGCAAGAGGAAGGATAG	NM_022415.3	150
<i>Hpgds/HPGDS</i>	TGGGAAGACAGCGTTGGAG	AGGCGAGGTGCTTCATGTG	NM_019455.4	147

Ccl2, C-C motif chemokine ligand 2; Cxcl1/2, C-X-C motif chemokine ligand 1/2; Mgll, monoglyceride lipase; Piges, prostaglandin E synthase.

with the amplicon size. We report in Supplemental Table S1 the basal expression of the measured genes.

Primary alveolar macrophages isolation and assay

Murine alveolar macrophages were recovered from the BAL as described by Zhang *et al.* (27) with slight modifications. Briefly, 7–8-wk-old CD1 mice were anesthetized and then euthanized by cervical dislocation. After a surgical incision, the trachea was exposed, and a cannula was fixed in it. Five consecutive lung lavages were performed through this cannula with 1 ml of PBS-EDTA (0.5 mM). The alveolar cells recovered were pelleted by centrifugation at 250 g for 5 min at 4°C, resuspended in culture medium [Roswell Park Memorial Institute (RPMI) 1640 medium supplemented with 10% fetal bovine serum and antibiotics], and counted in Turk's solution (2×10^5 cells per well for the mRNA and ELISA; 10^6 cells per condition for lipid quantification). Three hours after the initial plating, the medium was renewed to remove nonadherent cells. The remaining cells were seeded overnight, and the experiments were performed the next day. As previously described (18, 24), cells were incubated with fresh culture medium containing the compounds of interest for 1 h, and then LPS or LTA was added for a final concentration of 100 ng/ml and 10 μ g/ml, respectively, and incubated as specified in the figure legends. During each experiment, a control condition was performed corresponding to cells only incubated with vehicle (DMSO, 0.1%) in the absence of LPS.

Neutrophil enrichment and assay

Murine neutrophils were isolated from bone marrow and BAL using a discontinuous density gradient as previously described by Swamydas *et al.* (28). Briefly, 7–8-wk-old CD1 mice were anesthetized and then euthanized by cervical dislocation. For bone marrow neutrophil recovery, cells were isolated from femurs and tibias. For bronchoalveolar neutrophil recovery, a lung lavage was performed on the mice, as previously described, 24 h after intratracheal administration of LPS (30 μ l/mouse at a concentration of 200 μ g/ml).

The cell suspensions obtained were centrifuged at 300 g for 5 min, and red blood cells were removed by hypotonic lysis. Next, resuspended cells were carefully loaded on a Percoll gradient composed of 2 solutions of differential density (1.119 and 1.077) and centrifuged at 700 g for 30 min without using a brake. Neutrophils were collected on the interface layer, resuspended in RPMI 1640 medium supplemented with bovine serum albumin (0.025%), and counted with Turk's solution (10^6 cells per well). Cells were incubated with medium containing the compounds of interest and LPS at a final concentration of 100 ng/ml for 4 h. During each experiment, a control condition was performed, corresponding to cells only incubated with vehicle (DMSO, 0.1%) in the absence of LPS.

2-AG and lysophospholipid quantification

We quantified 2-AG and lysophospholipids by high performance liquid chromatography coupled to mass spectrometry (HPLC-MS) using a Linear Trap Quadrupole (LTQ)-Orbitrap Mass Spectrometer (Thermo Fisher Scientific). For quantification in lungs, the inferior lobe of the right lung was weighed and stored at -80°C directly after euthanasia. For alveolar macrophages (10^6 cells per condition), following incubation, medium was removed, and cells were recovered by scraping using PBS. Lungs or cells were homogenized in a glass vial containing dichloromethane (8 ml). Following internal standard addition (d_5 -2AG for 2-AG and 17:1 lysoPI, 17:1 lysoPS, 17:0 lysoPC, 17:0 lysoPE,

and 17:1 lysoPG for the lysophospholipids), lipid extraction was achieved by adding methanol (4 ml), water (2 ml), and HCl 2N (300 μ l). For the BAL samples, we used the same procedure, but used 16 and 8 ml of dichloromethane and methanol, respectively. To avoid autoxidation, butylated hydroxytoluene (10 μ g) and EDTA (20 ng) were added to the mixture. Vials were then shaken vigorously and sonicated. After centrifugation, the organic phase was recovered and evaporated under a nitrogen stream. Samples were prepurified by solid-phase extraction using unbounded silica as the stationary phase. Following a washing step, 2-AG was recovered with hexane-isopropanol (7:3; v/v), whereas lysophospholipids were subsequently eluted using methanol.

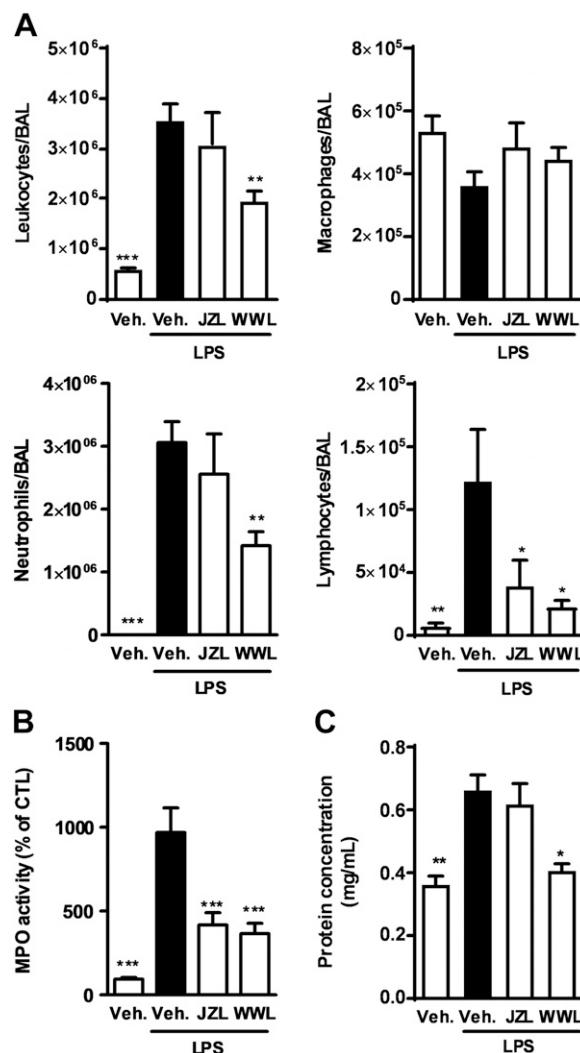


Figure 1. Effect of the ABHD6 inhibitor WWL70 and the MAGL inhibitor JZL184 on leukocyte recruitment in the lungs. ALI was induced by intratracheal instillation of LPS (6 μ g/mouse). The MAGL inhibitor JZL184 (JZL, 16 mg/kg), the ABHD6 inhibitor WWL70 (WWL, 20 mg/kg), or vehicle (Veh.) was administered intraperitoneally 1 h prior to LPS. Inflammatory parameters were evaluated 24 h after LPS administration. **A)** Cellular parameters were assessed by morphologic counting after cytopspin and a Diff-Quik coloration. Total and differential (macrophages, neutrophils, and lymphocytes) cell counts were performed on BAL fluid 24 h after LPS instillation. **B)** MPO activity was measured to assess tissue infiltration by neutrophils. Results are expressed as the percentage of the control (CTL) condition (Veh.). **C)** The total protein concentrations were measured in the BAL to evaluate the capillary leakage. Data are means \pm SEM; $n = 8$ mice/group. * $P < 0.05$, ** $P < 0.01$, *** $P < 0.001$ vs. the LPS-veh group.

After evaporation under a nitrogen stream, all the samples were reconstituted with methanol for injection of 25 μ l on the HPLC-MS system. The levels of lysophosphatidic acids were not quantifiable in our settings.

We analyzed the 2-AG containing fractions in positive mode as previously reported by Mutemberezi *et al.* (29). We analyzed the lysophospholipid fraction with the same mass spectrometer but used in negative ionization mode with an electrospray source (20). The data analysis was performed using Xcalibur software from Thermo Fisher Scientific. For each lipid, the signal (area under the curve) was normalized using the signal obtained for the corresponding internal standard and, for the lungs, based on the tissue weight.

Prostaglandin quantification

We quantified prostaglandin E2 (PGE₂) and prostaglandin D2 (PGD₂) using a ultra-performance liquid chromatography (UPLC) system coupled to a Xevo-TQ-S Mass Spectrometer (Waters, Milford, MA, USA). The inferior lobe of the right lung was weighed and stored at -80°C directly after euthanasia. For prostaglandin extraction, the tissue was homogenized in chloroform (8 ml), and the internal standard deuterated PGE₂ (d₅-PGE₂) was subsequently added. Then, methanol containing butylated hydroxytoluene (4 ml) and water containing EDTA (2 ml) were added to the vials before shaking and incubating them in an ice-cold ultrasonic water bath. After centrifugation, the organic layer was recovered and evaporated to dryness under nitrogen. Samples were reconstituted and loaded on a silica column for solid-phase extraction. Following a washing step, the prostaglandins were eluted

using CHCl₃ and methanol (8:2, v/v), and the resulting fraction was brought to dryness under a nitrogen stream. The residue was reconstituted in acetonitrile-water prior to its analysis as previously described in Alhouayek *et al.* (30). For data acquisition and processing, the MassLynx software (Waters) was used. For each prostaglandin, the signal (area under the curve) was normalized using the signal obtained for d₄-PGE₂ and based on the tissue weight.

Statistical analysis

Prism v.5.0 (GraphPad Software, La Jolla, CA, USA) was used for statistical analysis. Results are expressed as means \pm SEM. Differences between groups were assessed by 1-way ANOVA followed by a Dunnett's *post hoc* test or an unpaired Student's *t* test as parametric test, and a Kruskal-Wallis test followed by the Dunn's *post hoc* test with the untreated LPS (LPS-veh) group as the control or Mann-Whitney as nonparametric test. Statistical significance was taken when $P < 0.05$.

RESULTS

The ABHD6 inhibitor WWL70, but not the MAGL inhibitor JZL184, decreases leukocyte recruitment in the lungs

To investigate the effect of MAGL and ABHD6 inhibition on lung inflammation, we used a model of ALI induced by intratracheal instillation of LPS. This model induces a

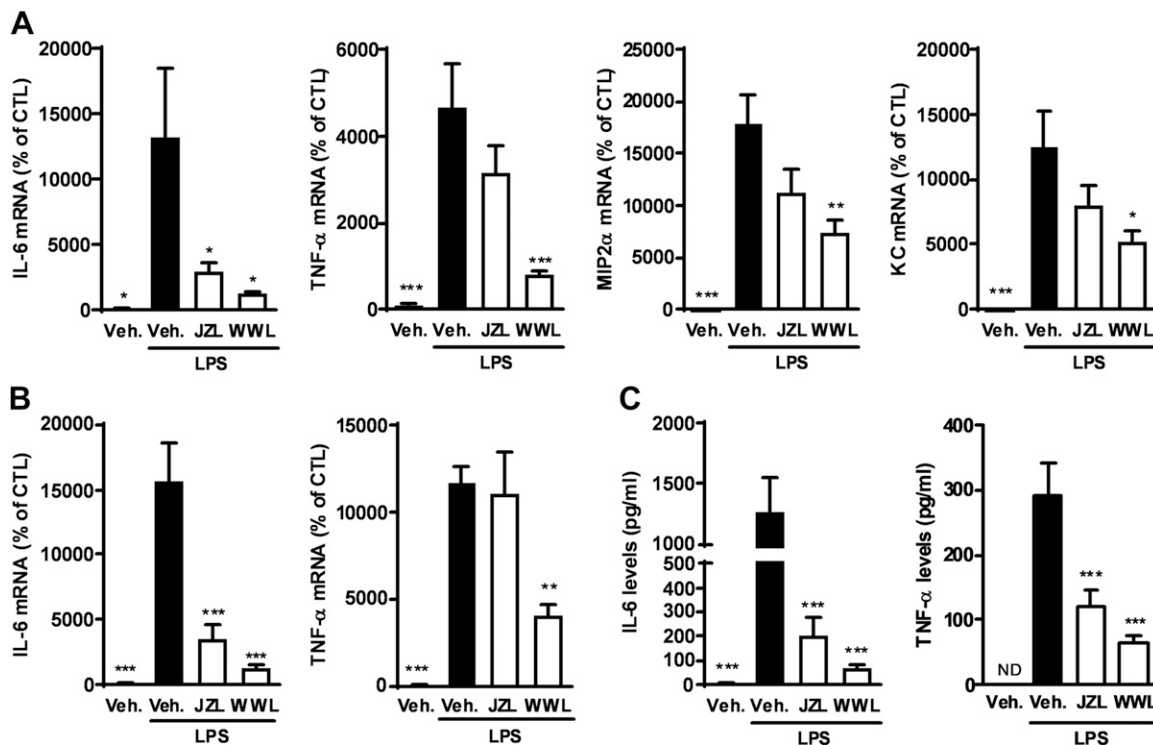


Figure 2. Effect of the ABHD6 inhibitor WWL70 and the MAGL inhibitor JZL184 on the proinflammatory markers of lung inflammation. ALI was induced by intratracheal instillation of LPS (6 μ g/mouse) for 24 h. The MAGL inhibitor JZL184 (JZL, 16 mg/kg), the ABHD6 inhibitor WWL70 (WWL, 20 mg/kg), or vehicle (Veh.) was administered intraperitoneally 1 h prior to LPS. A) mRNA expression of proinflammatory cytokines (TNF- α and IL-6) and chemokines (MIP2 α and KC) was measured by qRT-PCR using RPL19 as reference gene in the lungs. B) Proinflammatory cytokine expression was measured in the cells recovered from the BAL fluid by qPCR using RPL19 as reference gene. The results are relative to the control (CTL) group (Veh.) set at 100%. C) Proinflammatory cytokine production was measured in the BAL fluid by ELISA. Results are expressed in pg/mL. Data are means \pm SEM; $n = 8$ mice/group. * $P < 0.05$, ** $P < 0.01$, *** $P < 0.001$ vs. the LPS-veh group.

recruitment of leukocytes in the lungs. Following LPS administration, the total number of inflammatory cells in the BAL fluid was increased for mice receiving LPS compared with control mice. This was mainly due to an increase in the number of neutrophils (Fig. 1A), although the number of lymphocytes was also significantly increased (Fig. 1A). In this model, intratracheal instillation of LPS induced a decrease of ABHD6 mRNA expression in the lungs, whereas MAGL expression remained unchanged (Supplemental Fig. S1A). Prostaglandins are important players in lung inflammation. Here, we found that LPS induces an increase of microsomal prostaglandin E synthase 1 (mPGES1) mRNA expression, whereas hematopoietic prostaglandin D synthase (HPGDS) expression was unaffected (Supplemental Fig. S1A).

The ABHD6 inhibitor, WWL70 (20 mg/kg, i.p.) (18, 31), and the MAGL inhibitor, JZL184 (16 mg/kg, i.p.) (32), were administered to mice 1 h before LPS instillation. Treatment with WWL70 significantly decreased the total cell number present in the BAL fluid as well as the number of neutrophils and lymphocytes compared with the LPS-veh group (Fig. 1A). Contrary to WWL70, JZL184 had no effect on leukocyte, macrophage, and neutrophil recruitment in the BAL fluid. However, the number of lymphocytes was decreased with the MAGL inhibitor (Fig. 1A).

We also measured the MPO activity, a marker for neutrophil recruitment, in the lung to assess the degree of neutrophil infiltration in the tissue itself. Twenty-four hours post-LPS instillation, MPO activity was increased when compared with control mice. Interestingly, both the ABHD6 inhibitor and the MAGL inhibitor decreased MPO activity compared with the

LPS-veh group (Fig. 1B). This decrease of MPO activity with JZL184 could reflect a decrease of neutrophil presence in the lung tissue itself, although the MAGL inhibitor did not decrease neutrophil numbers in the BAL fluid.

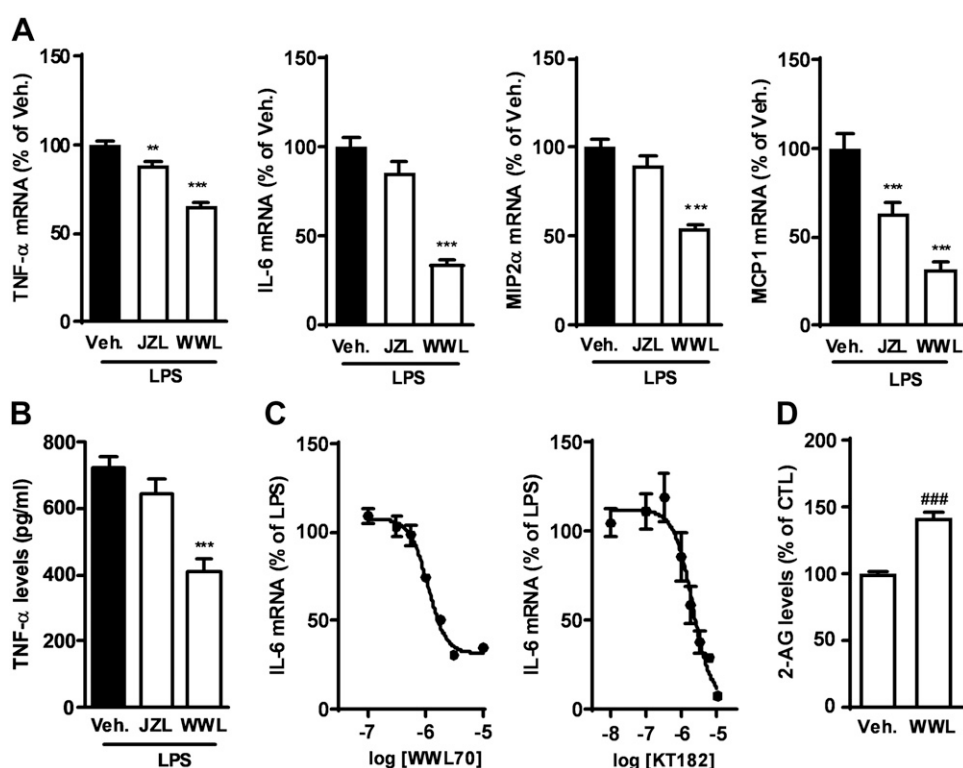
To evaluate the extent of capillary leakage resulting from the inflammatory reaction, the concentration of total proteins was measured in the BAL fluid. We observed an increase in protein concentration for the LPS-veh group compared with control mice that was decreased by the administration of WWL70, but not by JZL184 (Fig. 1C).

Both the ABHD6 inhibitor and the MAGL inhibitor decreased proinflammatory markers in the lungs

To evaluate the inflammatory reaction triggered in this ALI model, we analyzed the expression of inflammatory markers using qPCR in the lung tissue 24 h post-LPS. In the LPS-veh group, mRNA expression of proinflammatory cytokines such as TNF- α and IL-6, and of chemokines such as macrophage inflammatory protein 2 α (MIP2 α) and keratinocyte chemokine (KC), was increased compared with control mice (Fig. 2A). The administration of WWL70 reduced the mRNA expression of these cytokines and chemokines (Fig. 2A). However, for the mice receiving JZL184, there were no statistically significant variations except for IL-6 expression (Fig. 2A).

Next, we measured mRNA expression of IL-6 and TNF- α in the cells recovered from the BAL. As seen in the tissue itself, there was an increase in the mRNA expression of these cytokines in the LPS-veh group compared with

Figure 3. Effect of ABHD6 and MAGL inhibition on LPS-induced activation of primary alveolar macrophages. Cells were preincubated with vehicle (Veh., DMSO 0.1%) or the enzyme inhibitors for 1 h before stimulation with LPS (100 ng/ml) for 8 h. A) mRNA expression of proinflammatory cytokines (TNF- α and IL-6) and chemokines (MIP2 α and MCP1) was measured by qRT-PCR with RPL19 as reference gene. B) TNF- α production was measured in the cell culture medium by ELISA. C) Two different ABHD6 inhibitors, WWL70 and KT182, dose-dependently decrease LPS-induced IL-6 mRNA expression measured by qPCR with RPL19 as reference gene. D) 2-AG levels in primary alveolar macrophages incubated with vehicle or WWL70 (WWL, 10 μ M) for 6 h. For A, C, and D, results are expressed as a percentage of the respective vehicle (Veh.) set at a 100%. For ELISA, results are expressed in pg/mL. Data represent means \pm SEM from 3 separate experiments in triplicate. ** P < 0.01, *** P < 0.001 *vs.* the LPS-veh group; ### P < 0.001 *vs.* control (CTL) condition.



control mice that was decreased by the ABHD6 inhibitor. The administration of JZL184 was able to reduce IL-6 mRNA expression but had no effect on TNF- α (Fig. 2B).

The levels of proinflammatory cytokines were also measured by ELISA in the BAL fluid. The secretion of IL-6 and TNF- α in the alveolar space was increased in the LPS-veh group compared with control mice. A decrease in the production of these 2 cytokines was observed in mice receiving WWL70 as well as JZL184 (Fig. 2C).

Effects of ABHD6 and MAGL inhibition on LPS-activated primary alveolar macrophages and neutrophils

As mentioned, alveolar macrophages are key regulators of lung inflammation because they serve as the first line of cellular defense against pathogens. Decreasing their activation could therefore limit ALI. We thus wanted to investigate, *in vitro*, the consequences of ABHD6 and MAGL inhibition on LPS-induced macrophage activation. Therefore, we recovered primary alveolar macrophages from the BAL of naive mice and incubated them with LPS for 8 h. LPS-activated macrophages had an increase in mRNA expression of proinflammatory markers such as TNF- α , IL-6, MIP2 α , and monocyte chemoattractant protein 1 (MCP1) compared with control alveolar macrophages (Supplemental Fig. S1B, C). The mRNA expression of MAGL and HPGDS was decreased in activated cells, whereas it was increased for ABHD6 and mPGES1 (Supplemental Fig. S1D). Inhibiting ABHD6 with WWL70 in LPS-activated alveolar macrophages lowered cell activation by decreasing expression of these proinflammatory cytokines (IL-6 and TNF- α) and chemokines (MIP2 α and MCP1) (Fig. 3A–C) and, as expected, it increased 2-AG levels (Fig. 3D).

Although JZL184 decreased TNF- α and MCP1 mRNA, it had no effect on LPS-induced IL-6 and MIP2 α mRNA expression (Fig. 3A). To further support ABHD6 involvement, we treated alveolar macrophages with increasing concentrations of WWL70 and a second ABHD6 inhibitor, KT182 (33). As shown in Fig. 3C, both ABHD6 inhibitors dose-dependently decreased LPS-induced IL-6 mRNA expression in alveolar macrophages. In this setting, the obtained half-maximal inhibitory concentration values were 1.1 and 2 μ M for WWL70 and KT182, respectively.

As mentioned previously, neutrophils are implicated in the severity of ALI. To explore the potential implication of neutrophils in the effects of ABHD6 inhibition, we incubated, *in vitro*, the cells with LPS to induce their activation and thus the production of proinflammatory cytokines (Supplemental Fig. S1E, F). Using this protocol, we showed that inhibiting ABHD6 with WWL70 slightly decreased TNF- α and IL-6 production in LPS-activated neutrophils isolated from the alveolar space of inflamed mice (Fig. 4A). When using a neutrophil-enriched cell population recovered from the bone marrow, WWL70 treatment reduced only TNF- α (Fig. 4B). Interestingly, inhibiting MAGL with JZL184 in the same LPS-activated neutrophil populations had no effect on cytokine levels when cells were recovered from the BAL. Nevertheless, in LPS-activated neutrophils derived from bone marrow, JZL184 increased TNF- α and lowered IL-6 production (Fig. 4).

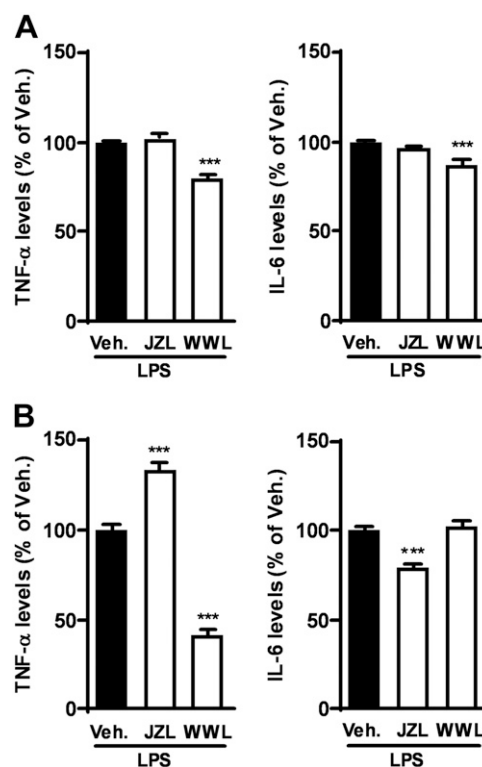


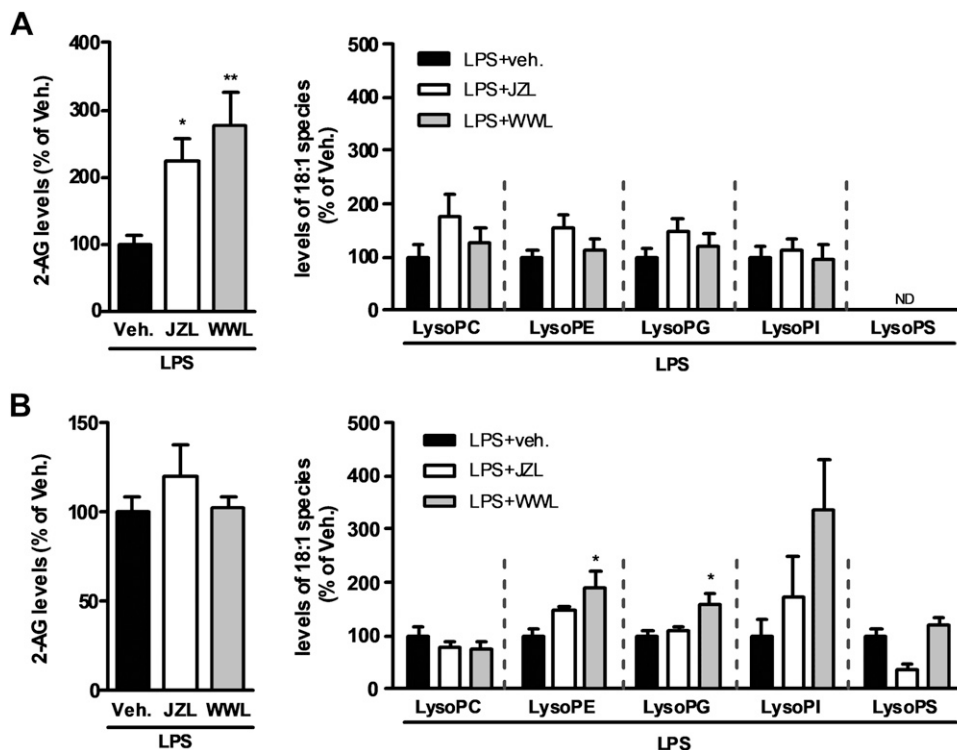
Figure 4. Effect of ABHD6 and MAGL inhibition on LPS-induced activation of a neutrophil-enriched cell population recovered from bone marrow or BAL. Neutrophils from BAL (A) and bone marrow (B) were coincubated with vehicle (Veh., DMSO 0.1%) and LPS (100 ng/ml), or LPS and the enzyme inhibitors (10 μ M) for 4 h. Production of proinflammatory cytokines (TNF- α and IL-6) was measured in the cell culture medium by ELISA. Results are expressed as a percentage of the effect of LPS set at a 100%. Data represent means \pm SEM. *** P < 0.001 vs. the LPS-veh group.

Effect of WWL70 on the substrates of ABHD6 in lungs and alveolar macrophages

We showed that ABHD6 inhibition by WWL70 decreases LPS-induced lung inflammation and alveolar macrophage activation. In order to generate some hypotheses on the mechanism of action, we quantified by HPLC-MS the levels of the substrates of ABHD6 (*i.e.*, 2-AG and lysophospholipids) (15, 19, 20) in the lung, the BAL fluid, and alveolar macrophages.

ABHD6 and MAGL inhibition in the ALI model increased the levels of 2-AG in the BAL fluid 25 h after drug administration compared with the LPS-veh group (Fig. 5A), whereas in the lung tissue, neither JZL184 nor WWL70 increased 2-AG levels (Fig. 5B). To confirm that ABHD6 inhibition could increase 2-AG levels in the lung tissue, we measured the levels at an earlier time point (*i.e.*, 6 h) and found increased 2-AG levels following ABHD6 and MAGL inhibition (Supplemental Fig. S1G, H). When looking at the oleoyl-containing lysophospholipids, [*i.e.*, the lysophospholipids biochemically characterized as ABHD6 substrates by Thomas *et al.* (19)], we found significantly increased levels of 18:1 lysoPG and 18:1 lysoPE in the lungs 25 h (but not 6 h, Supplemental Table S2).

Figure 5. Effect of ABHD6 inhibition by JZL184 and WWL70 on 2-AG and lysophospholipid levels in the BAL fluid and in the lungs. ALI was induced by intratracheal instillation of LPS (6 μ g/mouse). The MAGL inhibitor JZL184 (JZL, 16 mg/kg), the ABHD6 inhibitor WWL70 (WWL, 20 mg/kg), or vehicle (Veh.) were administered intraperitoneally 1 h prior to LPS. 2-AG and lysophospholipid levels were measured by HPLC-MS in the BAL fluid (A) and in the lungs (B) 24 h after LPS instillation. The full set of data for lysophospholipids is available in Supplemental Tables S2 and S3. Data are means \pm SEM and expressed as a percentage of the control condition (Veh.); $n = 8$ mice/group. * $P < 0.05$, ** $P < 0.01$ vs. the LPS-veh group. LysoPA was not detected (ND).



post-WWL70 administration (Fig. 5B). The levels of 18:1 lysoPI, 18:1 lysoPS, and 18:1 lysoPC remained unaltered (Fig. 5B). In the BAL fluid, no variation was observed for the 18:1 lysophospholipids (Fig. 5A). The situation is more complex, however, when looking, beyond the 18:1 lysophospholipids, at all the lysophospholipids detected by our method because the majority of lysophospholipids were not increased in our experimental settings in the lungs (Supplemental Table S2) and in the alveolar space (Supplemental Table S3) when mice received WWL70.

In the alveolar macrophages, incubation with WWL70 for 6 h did not result in increased lysophospholipid levels in control conditions or in the presence of LPS, except for 22:5 lysoPG, 22:6 lysoPG, and 20:4 lysoPC (Supplemental Table S4).

Besides the substrates of ABHD6, we thought to quantify PGE₂ in the lungs of mice treated with WWL70. Indeed, a recent study suggested ABHD6-independent effects for WWL70 *via* the inhibition of mPGES 1 and 2 (mPGES1/2) and thus decreased production of PGE₂ (34). Because in the LPS-treated animal the anti-inflammatory effects of WWL70 would have masked a potential direct effect of WWL70 on mPGES1/2, we decided to assess whether administration of WWL70 (20 mg/kg, i.p.) could inhibit PGE₂ production in lungs from control mice. Surprisingly, we observed an increase in PGE₂ levels in the WWL70 group 6 h after injection, compared with the control group, which strongly suggested that, in our conditions, the effects of WWL70 were independent of mPGES1/2 inhibition (Supplemental Fig. S1I). Of note, the levels of prostaglandin D₂, measured in the same settings, were not altered by WWL70 treatment (Supplemental Fig. S1I).

2-AG and some lysophospholipid species decrease LPS-induced activation of primary alveolar macrophages

We have shown that ABHD6 inhibition decreases alveolar macrophage activation. Therefore, we decided to investigate whether the suggested substrates of ABHD6 would decrease LPS-induced alveolar macrophage activation. Primary alveolar macrophages from CD1 mice were therefore incubated in the presence of LPS and 2-AG, lysoPC, lysoPG, lysoPE, lysoPI, or lysoPS for 8 h. We found that 2-AG decreases the LPS-induced increase in mRNA expression of proinflammatory cytokines (IL-6, IL-1 β , and TNF- α) but failed to decrease MIP2 α expression (Fig. 6).

Concerning the lysophospholipids, we observed differences in the effects depending on the lysophospholipid family tested. LysoPI had no significant effects on IL-1 β , TNF- α , and MIP2 α , but decreased IL-6 expression. LysoPS decreased IL-1 β and TNF- α , but not IL-6 or MIP2 α . LysoPC and lysoPE had the same effect on the markers studied because they only decreased IL-1 β , whereas lysoPG had no effect on IL-1 β , TNF- α , and MIP2 α , but increased IL-6 mRNA expression (Fig. 6).

The ABHD6 inhibitor WWL70 has beneficial effects when given as treatment

Because we had interesting results on alveolar macrophages and in our previous study when WWL70 was administered 1 h before LPS instillation (and thus ALI development), we decided to assess the effect of ABHD6 inhibition when the inhibitor is given after the initiation of inflammation. Therefore, we administered WWL70 1 h after LPS administration, when inflammatory processes

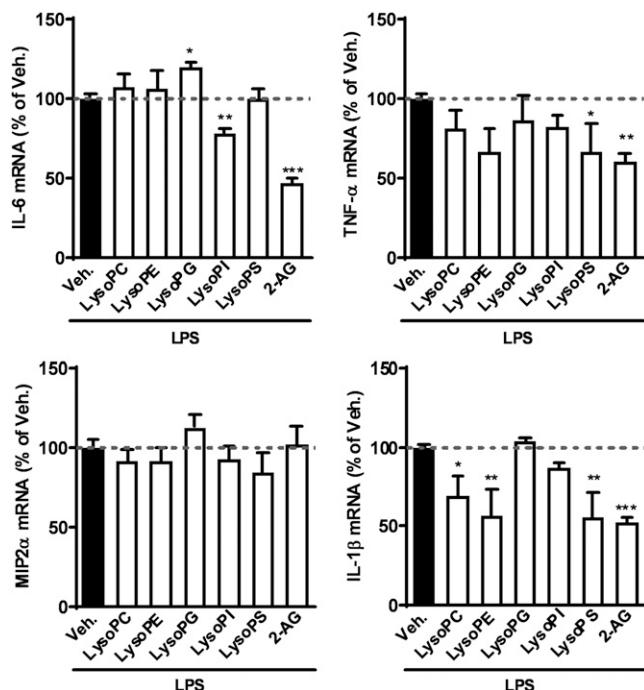


Figure 6. Effect of 2-AG and lysophospholipids on LPS-induced activation of primary alveolar macrophages. Cells were preincubated with vehicle (Veh., DMSO 0.1%), 2-AG (10 μ M), or different lysophospholipids (10 μ M) for 1 h before stimulation with 100 ng/ml of LPS for 8 h. mRNA expression of proinflammatory cytokines (TNF- α , IL-6, and IL-1 β) and chemokine (MIP2 α) was measured by qPCR with RPL19 as reference gene. Results are expressed as a percentage of the effect of LPS set at a 100%. Data represent the mean \pm SEM from 3 separate experiments in triplicate. * P < 0.05, ** P < 0.01, *** P < 0.001 *vs.* the LPS-veh group.

have started (21). As for the previous study, we evaluated the inflammatory parameters 24 h after intratracheal instillation of LPS.

As in the previous experiment, WWL70 decreased leukocyte recruitment by half in the alveolar space. This is mainly due to a reduced trafficking of neutrophils and, to a lesser extent, a reduction in the number of lymphocytes (Fig. 7A). In this treatment scheme, WWL70 also reduced MPO activity (Fig. 7B) as well as protein concentration in the BAL fluid (Fig. 7C), which reflects a reduction of the microvascular leakage induced by intratracheal administration of LPS. Proinflammatory cytokine (IL-6 and TNF- α) and chemokine (MIP2 α and KC) mRNA expression was decreased in the lung tissue itself following WWL70 administration (Fig. 8A). Moreover, inhibiting ABHD6 reduced the activation of cells present in the alveolar space, as illustrated by a decrease in IL-6 and TNF- α expression in these cells (Fig. 8B), and lowered the levels of TNF- α and IL-6 secreted in the BAL fluid (Fig. 8C).

Effects of ABHD6 inhibition on LTA-activated primary alveolar macrophages

Because it was shown that, in humans, activation of TLR2 or TLR4 results in differential pulmonary inflammation (35), we thought to assess the effect of

ABHD6 inhibition on primary alveolar macrophages activated through the TLR2-signaling pathway. As performed previously, cells were preincubated with WWL70 for 1 h before stimulation with LTA. Inhibiting ABHD6 with WWL70 decreased both TNF- α and IL-6 mRNA expression induced by LTA (Fig. 9).

DISCUSSION

Inflammation is a key element of many pulmonary diseases. Although many strategies have been explored,

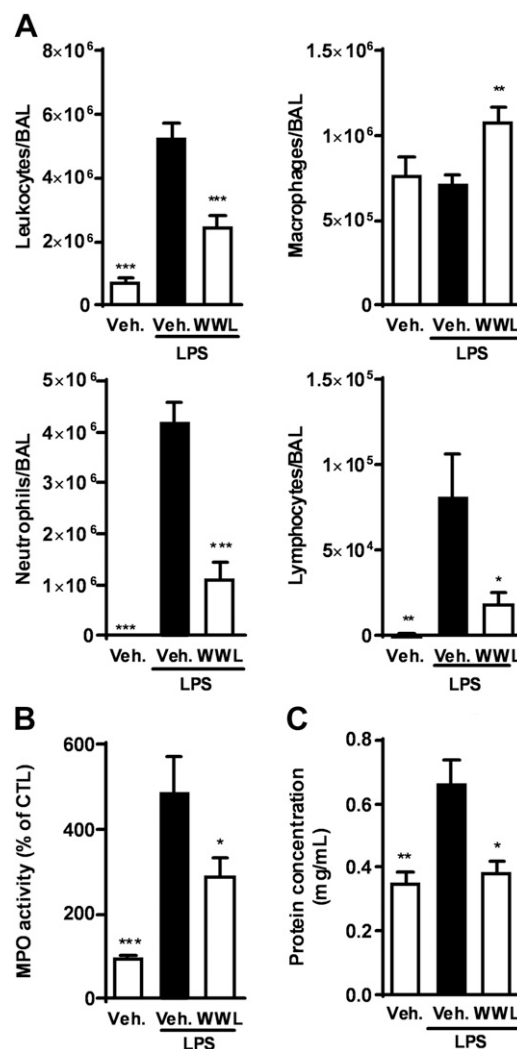
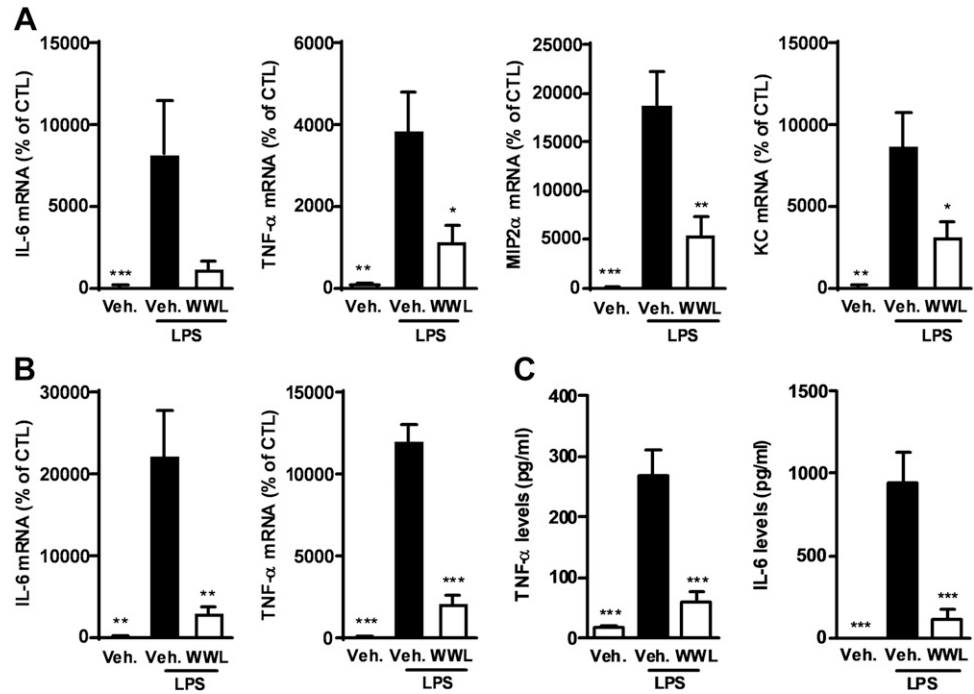


Figure 7. Therapeutic effect of the ABHD6 inhibitor WWL70 on ALI induced by intratracheal instillation of LPS. ALI was induced by intratracheal instillation of LPS (6 μ g/mouse). The ABHD6 inhibitor WWL70 (WWL, 20 mg/kg) or vehicle (Veh.) was administered intraperitoneally 1 h after LPS. Inflammatory parameters were evaluated 24 h after LPS administration. A) Total and differential (macrophages, neutrophils, and lymphocytes) cell counts were performed in BAL fluid by morphologic counting after cytopsin and a Diff-Quik coloration. B) MPO activity was measured in lung tissue homogenates and expressed as a percentage of the control (CTL) condition (Veh.). C) The total protein concentration was measured in the BAL fluid to evaluate the capillary leakage. Data are means \pm SEM; n = 8 mice/group. * P < 0.05, ** P < 0.01, *** P < 0.001 *vs.* the LPS-veh group.

Figure 8. Therapeutic effect of the ABHD6 inhibitor WWL70 on proinflammatory markers of lung inflammation. ALI was induced by intratracheal instillation of LPS (6 μ g/mouse). The ABHD6 inhibitor WWL70 (WWL, 20 mg/kg) or vehicle (Veh.) was administered intraperitoneally 1 h after LPS. **A)** mRNA expression in the lungs of proinflammatory cytokines (TNF- α and IL-6) and chemokines (MIP2 α and KC) was measured by qPCR with RPL19 as reference gene. **B)** Proinflammatory cytokine mRNA expression was measured in the cells recovered from the BAL fluid by qPCR with RPL19 as reference gene. Results are relative to the control group (CTL) set at 100% (A, B). **C)** Proinflammatory cytokine production was measured in the BAL fluid by ELISA and is expressed in pg/mL. Data are means \pm SEM; $n = 8$ mice/group. * $P < 0.05$, ** $P < 0.01$, *** $P < 0.001$ vs. the LPS-veh group.



tackling inflammation is still complex in lung pathologies. The endocannabinoid system is described to be involved in inflammatory processes; nevertheless, little is known about the effects of 2-AG and the inhibition of ABHD6 in lung inflammation (12).

In the present study, we provided evidence to support the role of ABHD6 inhibition in counteracting the inflammatory insult induced by intratracheal instillation of LPS. Indeed, administration of the ABHD6 inhibitor WWL70 reduced leukocytes and, more precisely, neutrophil and lymphocyte recruitment in the alveolar space, microvascular leakage, and neutrophil migration in the tissue itself. Moreover, WWL70 also reduced production of proinflammatory cytokines and chemokines. Similar effects were observed when WWL70 was given as treatment 1 h after induction of inflammation. In our experimental settings, the MAGL inhibitor JZL184 also had anti-inflammatory properties [as previously reported by Costola-de-Souza *et al.* (14)] but was less efficient in protecting against pulmonary inflammation because it decreased fewer markers of ALI compared with WWL70.

Alveolar macrophages are described to be key regulators of the initiation and resolution of lung inflammation. We previously showed that WWL70 and 2-AG decreased LPS-induced macrophage activation on cell lines in culture and mouse peritoneal macrophages (18). Here, we extended these findings to mouse primary alveolar macrophages obtained from BAL fluid. Moreover, the effects of WWL70 were not limited to TLR4 activation because the ABHD6 inhibitor also reduced LTA-induced macrophage activation. Although alveolar macrophages are key players in ALI,

other cell types are implicated in this inflammatory process, such as neutrophils. Incubation of WWL70 with neutrophils decreased their LPS-induced activation. Although additional studies might be necessary to further characterize the consequences of ABHD6 inhibition on neutrophil activation, recruitment, and degranulation, our data suggest that neutrophils are implicated in the ability of WWL70 to decrease lung inflammation *in vivo*.

When using enzyme inhibitors, a key question is what substrate or product of the enzyme is responsible for the

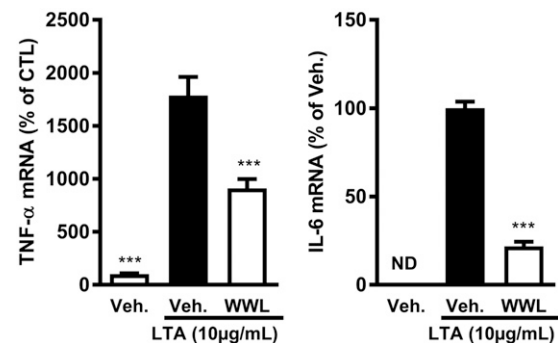


Figure 9. Effect of ABHD6 inhibition on LTA-induced activation of primary alveolar macrophages. Cells were preincubated with vehicle (Veh., DMSO 0.1%) or the ABHD6 inhibitor WWL70 (WWL, 10 μ M) for 1 h before stimulation with LTA (10 μ g/mL) for 8 h. mRNA expression of proinflammatory cytokines was measured by qPCR using RPL19 as reference gene. Results are expressed as a percentage of the effect of control (CTL) or LTA set at a 100%. ND, not detected. Data represent the mean \pm SEM. ** $P < 0.01$, *** $P < 0.001$ vs. the LTA-activated untreated group.

observed effect. Because recent studies proposed new substrates such as lysophospholipids for ABHD6 (19), we quantified by HPLC-MS the levels of these lipids in the lung following ABHD6 inhibition. 2-AG levels were increased in the lungs 6 h after WWL70 administration and in the alveolar space after 24 h. This is consistent with the increase in 2-AG levels 4 h after WWL70 injection as we previously observed in the lungs in a model of systemic inflammation induced by intraperitoneal administration of LPS (18). 16:0 LysoPG and 18:1 lysoPG levels were increased at 24 h but not at 6 h after treatment. This is in accordance with recent findings that suggest a lower velocity for lysoPG than for monoacylglycerol hydrolysis by ABHD6 (36). Although MAGL has never been described as a lysophospholipase, we also show variations in the levels of some lysophospholipids in the alveolar space (but not in the lungs) 24 h after JZL184 administration. Additional studies are required to determine whether these observations are a direct or indirect consequence of MAGL inhibition.

The early increase in 2-AG levels following ABHD6 inhibition could explain the decrease of alveolar macrophage activation and thus lung inflammation. These results, however, do not exclude the potential implication of lysophospholipids in the beneficial effects of WWL70 on pulmonary insult, although we were not able to clearly show an increase in their levels in our experimental settings. Indeed, although the biologic effects of lysophospholipids remain to be fully understood, these lipids are described to be implicated in inflammatory processes (37, 38). Here, following ABHD6 inhibition, the levels of some species of lysophospholipids were increased. This is consistent with what was reported by Thomas *et al.* (19) *in vivo* and by our group in J774 cells (20). LysoPGs were reported to inhibit chemotactic migration and IL-1 β production by phagocytes (39). Orally administered lysoPEs were shown to reduce proinflammatory markers in a model of murine peritonitis (40). However, although some effects have been described for lysophospholipids, we did not observe a clear effect on LPS-induced primary alveolar macrophage activation. Thus, our data suggest that in alveolar macrophages, most of the effects of ABHD6 inhibition are due to 2-AG. *In vivo*, it could be more complicated, because lysophospholipids could act through another mechanism or act in a synergistic way with 2-AG to decrease pulmonary inflammation. For instance, lysoPI were previously shown to modulate the effect of 2-AG on inflammation. Indeed, lysoPI potentiated neutrophil migration toward 2-AG. This was accompanied by the inhibition of neutrophil degranulation and reactive oxygen species generation (41). Further studies will be necessary to decipher their potential implication *in vivo* in this ALI model.

Finally, we also investigated the effect of WWL70 on PGE₂ levels. Indeed, recent studies suggested that the anti-inflammatory effects of WWL70 were partially due to an inhibition of mPGES1 and thus an attenuation of PGE₂ production (34). Surprisingly, in our hands, WWL70 administration increased PGE₂ levels in the lungs. Moreover, although PGE₂ is commonly described as a proinflammatory mediator, in the lung this prostaglandin is described to have anti-inflammatory properties and to

be implicated in tissue repair (42). Therefore, although the mechanism by which WWL70 increases PGE₂ levels is unclear, this could be part of its beneficial effects in lung inflammation.

In summary, we put forth ABHD6 inhibition with WWL70 as a potential therapeutic strategy in pulmonary diseases. Our working hypothesis is that ABHD6 inhibition exerts beneficial effects through an increase in 2-AG levels resulting in a decrease of macrophage and, potentially, neutrophil activation, and thus a decrease of the inflammatory process. The implication of lysophospholipids in this process remains to be fully investigated. **[F]**

ACKNOWLEDGMENTS

The authors thank H.P. Patil and C. Loira-Pastoriza from Dr. R. Vanbever's laboratory [Université Catholique de Louvain (UCLouvain)] for helpful discussions related to the mouse model, Dr. L. Dumoutier's laboratory (UCLouvain) for access to cytospin, and Dr. V. Mutemberezi (UCLouvain) for help with lipid quantification. The Mass Spectrometry of Metabolites (MASSMET) platform (UCLouvain) is acknowledged for access to the LC-MS. G.G.M. is the recipient of grants from the Fonds de la Recherche Scientifique (FRS-FNRS; Brussels, Belgium) and from the Fonds Spéciaux de Recherches (FSR; UCLouvain). P.B. is a research fellow of the Fonds pour la Recherche dans l'Industrie et l'Agriculture (FRIA; Brussels, Belgium). M.A. is a postdoctoral fellow from the FRS-FNRS. G.G.M. is the recipient of grants from the FRS-FNRS (PDR T.0148.14, CDR J.0084.18) and from the FSR. The authors declare no conflicts of interest.

AUTHOR CONTRIBUTIONS

P. Bottemanne, M. Alhouayek, and G. G. Muccioli designed research; P. Bottemanne, A. Paquot, H. Ameraoui, M. Alhouayek, and G. G. Muccioli performed experiments and analyzed data; P. Bottemanne, M. Alhouayek, and G. G. Muccioli wrote the manuscript; G. G. Muccioli supervised the whole study; and all authors read and approved the manuscript.

REFERENCES

1. Chen, H., Bai, C., and Wang, X. (2010) The value of the lipopolysaccharide-induced acute lung injury model in respiratory medicine. *Expert Rev. Respir. Med.* **4**, 773–783
2. Erickson, S. E., Martin, G. S., Davis, J. L., Matthay, M. A., and Eisner, M. D.; NIH NHLBI ARDS Network. (2009) Recent trends in acute lung injury mortality: 1996–2005. *Crit. Care Med.* **37**, 1574–1579
3. Rubenfeld, G. D., Caldwell, E., Peabody, E., Weaver, J., Martin, D. P., Neff, M., Stern, E. J., and Hudson, L. D. (2005) Incidence and outcomes of acute lung injury. *N. Engl. J. Med.* **353**, 1685–1693
4. Reutershan, J., and Ley, K. (2004) Bench-to-bedside review: acute respiratory distress syndrome - how neutrophils migrate into the lung. *Crit. Care* **8**, 453–461
5. Han, S., and Mallampalli, R. K. (2015) The acute respiratory distress syndrome: from mechanism to translation. *J. Immunol.* **194**, 855–860
6. Matute-Bello, G., Frevert, C. W., and Martin, T. R. (2008) Animal models of acute lung injury. *Am. J. Physiol. Lung Cell. Mol. Physiol.* **295**, L379–L399
7. Kopf, M., Schneider, C., and Nobs, S. P. (2015) The development and function of lung-resident macrophages and dendritic cells. *Nat. Immunol.* **16**, 36–44

8. Herold, S., Mayer, K., and Lohmeyer, J. (2011) Acute lung injury: how macrophages orchestrate resolution of inflammation and tissue repair. *Front. Immunol.* **2**, 65
9. Aggarwal, N. R., King, L. S., and D'Alessio, F. R. (2014) Diverse macrophage populations mediate acute lung inflammation and resolution. *Am. J. Physiol. Lung Cell. Mol. Physiol.* **306**, L709–L725
10. Buckley, C. D., Gilroy, D. W., Serhan, C. N., Stockinger, B., and Tak, P. P. (2013) The resolution of inflammation. *Nat. Rev. Immunol.* **13**, 59–66
11. Grommes, J., and Soehnlein, O. (2011) Contribution of neutrophils to acute lung injury. *Mol. Med.* **17**, 293–307
12. Alhouayek, M., Masquelier, J., and Muccioli, G. G. (2014) Controlling 2-arachidonoylglycerol metabolism as an anti-inflammatory strategy. *Drug Discov. Today* **19**, 295–304
13. Blankman, J. L., Simon, G. M., and Cravatt, B. F. (2007) A comprehensive profile of brain enzymes that hydrolyze the endocannabinoid 2-arachidonoylglycerol. *Chem. Biol.* **14**, 1347–1356
14. Costola-de-Souza, C., Ribeiro, A., Ferraz-de-Paula, V., Calefi, A. S., Aloia, T. P., Gimenes-Junior, J. A., de Almeida, V. I., Pinheiro, M. L., and Palermo-Neto, J. (2013) Monoacylglycerol lipase (MAGL) inhibition attenuates acute lung injury in mice. *PLoS One* **8**, e77706
15. Marrs, W. R., Blankman, J. L., Horne, E. A., Thomazeau, A., Lin, Y. H., Coy, J., Bodor, A. L., Muccioli, G. G., Hu, S. S., Woodruff, G., Fung, S., Lafourcade, M., Alexander, J. P., Long, J. Z., Li, W., Xu, C., Möller, T., Mackie, K., Manzoni, O. J., Cravatt, B. F., and Stella, N. (2010) The serine hydrolase ABHD6 controls the accumulation and efficacy of 2-AG at cannabinoid receptors. *Nat. Neurosci.* **13**, 951–957
16. Marrs, W. R., Horne, E. A., Ortega-Gutierrez, S., Cisneros, J. A., Xu, C., Lin, Y. H., Muccioli, G. G., Lopez-Rodriguez, M. L., and Stella, N. (2011) Dual inhibition of alpha/beta-hydrolase domain 6 and fatty acid amide hydrolase increases endocannabinoid levels in neurons. *J. Biol. Chem.* **286**, 28723–28728
17. Naydenov, A. V., Horne, E. A., Cheah, C. S., Swinney, K., Hsu, K. L., Cao, J. K., Marrs, W., Blankman, J. L., Tu, S., Cherry, A. E., Fung, S., Wen, A., Li, W., Saporito, M. S., Selley, D. E., Cravatt, B. F., Oakley, J. C., and Stella, N. (2014) ABHD6 blockade exerts antiepileptic activity in PTZ-induced seizures and in spontaneous seizures in R6/2 mice. *Neuron* **83**, 361–371
18. Alhouayek, M., Masquelier, J., Cani, P. D., Lambert, D. M., and Muccioli, G. G. (2013) Implication of the anti-inflammatory bioactive lipid prostaglandin D₂-glycerol ester in the control of macrophage activation and inflammation by ABHD6. *Proc. Natl. Acad. Sci. USA* **110**, 17558–17563
19. Thomas, G., Betters, J. L., Lord, C. C., Brown, A. L., Marshall, S., Ferguson, D., Sawyer, J., Davis, M. A., Melchior, J. T., Blume, L. C., Howlett, A. C., Ivanova, P. T., Milne, S. B., Myers, D. S., Mrak, I., Leber, V., Heier, C., Taschler, U., Blankman, J. L., Cravatt, B. F., Lee, R. G., Crooke, R. M., Graham, M. J., Zimmermann, R., Brown, H. A., and Brown, J. M. (2013) The serine hydrolase ABHD6 is a critical regulator of the metabolic syndrome. *Cell Reports* **5**, 508–520
20. Masquelier, J., Alhouayek, M., Terrasi, R., Botteman, P., Paquot, A., and Muccioli, G. G. (2018) Lysophosphatidylinositols in inflammation and macrophage activation: altered levels and anti-inflammatory effects. *Biochim. Biophys. Acta. Mol. Cell. Biol. Lipids* **1863**, 1458–1468
21. Bozinovski, S., Jones, J., Beavitt, S. J., Cook, A. D., Hamilton, J. A., and Anderson, G. P. (2004) Innate immune responses to LPS in mouse lung are suppressed and reversed by neutralization of GM-CSF via repression of TLR-4. *Am. J. Physiol. Lung Cell. Mol. Physiol.* **286**, L877–L885
22. Vernooij, J. H., Dentener, M. A., van Suylen, R. J., Buurman, W. A., and Wouters, E. F. (2001) Intratracheal instillation of lipopolysaccharide in mice induces apoptosis in bronchial epithelial cells: no role for tumor necrosis factor- α and infiltrating neutrophils. *Am. J. Respir. Cell Mol. Biol.* **24**, 569–576
23. Alhouayek, M., Lambert, D. M., Delzenne, N. M., Cani, P. D., and Muccioli, G. G. (2011) Increasing endogenous 2-arachidonoylglycerol levels counteracts colitis and related systemic inflammation. *FASEB J.* **25**, 2711–2721
24. Alhouayek, M., Botteman, P., Makriyannis, A., and Muccioli, G. G. (2017) N-acyl ethanolamine-hydrolyzing acid amidase and fatty acid amide hydrolase inhibition differentially affect N-acyl ethanolamine levels and macrophage activation. *Biochim. Biophys. Acta. Mol. Cell Biol. Lipids* **1862**, 474–484
25. Alhouayek, M., Botteman, P., Subramanian, K. V., Lambert, D. M., Makriyannis, A., Cani, P. D., and Muccioli, G. G. (2015) N-Acyl ethanolamine-hydrolyzing acid amidase inhibition increases colon N-palmitoylethanolamine levels and counteracts murine colitis. *FASEB J.* **29**, 650–661
26. De Berdt, P., Botteman, P., Bianco, J., Alhouayek, M., Diogenes, A., Llyod, A., Gerardo-Nava, J., Brook, G. A., Miron, V., Muccioli, G. G., and Rieux, A. D. (2018) Stem cells from human apical papilla decrease neuro-inflammation and stimulate oligodendrocyte progenitor differentiation via activin-A secretion. *Cell. Mol. Life Sci.* **75**, 2843–2856; erratum: 2857
27. Zhang, X., Goncalves, R., and Mosser, D. M. (2008) The isolation and characterization of murine macrophages. *Curr. Protoc. Immunol.* **Chapter 14**, Unit 14.1
28. Swamydas, M., Gao, J. L., Break, T. J., Johnson, M. D., Jaeger, M., Rodriguez, C. A., Lim, J. K., Green, N. M., Collar, A. L., Fischer, B. G., Lee, C. C., Perfect, J. R., Alexander, B. D., Kullberg, B. J., Netea, M. G., Murphy, P. M., and Lionakis, M. S. (2016) CXCR1-mediated neutrophil degranulation and fungal killing promote *Candida* clearance and host survival. *Sci. Transl. Med.* **8**, 322ra10
29. Mutemberezi, V., Masquelier, J., Guillemot-Legris, O., and Muccioli, G. G. (2016) Development and validation of an HPLC-MS method for the simultaneous quantification of key oxysterols, endocannabinoids, and ceramides: variations in metabolic syndrome. *Anal. Bioanal. Chem.* **408**, 733–745
30. Alhouayek, M., Buisseret, B., Paquot, A., Guillemot-Legris, O., and Muccioli, G. G. (2018) The endogenous bioactive lipid prostaglandin D₂-glycerol ester reduces murine colitis via DP1 and PPAR γ receptors. *FASEB J.* **32**, 5000–5011
31. Li, W., Blankman, J. L., and Cravatt, B. F. (2007) A functional proteomic strategy to discover inhibitors for uncharacterized hydrolases. *J. Am. Chem. Soc.* **129**, 9594–9595
32. Long, J. Z., Li, W., Booker, L., Burston, J. J., Kinsey, S. G., Schlosburg, J. E., Pavón, F. J., Serrano, A. M., Selley, D. E., Parsons, L. H., Lichtman, A. H., and Cravatt, B. F. (2009) Selective blockade of 2-arachidonoylglycerol hydrolysis produces cannabinoid behavioral effects. *Nat. Chem. Biol.* **5**, 37–44
33. Hsu, K. L., Tsuboi, K., Chang, J. W., Whitby, L. R., Speers, A. E., Pugh, H., and Cravatt, B. F. (2013) Discovery and optimization of piperidyl-1,2,3-triazole ureas as potent, selective, and in vivo-active inhibitors of α/β -hydrolase domain containing 6 (ABHD6). *J. Med. Chem.* **56**, 8270–8279
34. Tanaka, M., Moran, S., Wen, J., Affram, K., Chen, T., Symes, A. J., and Zhang, Y. (2017) WWL70 attenuates PGE₂ production derived from 2-arachidonoylglycerol in microglia by ABHD6-independent mechanism. *J. Neuroinflammation* **14**, 7
35. Hoogerwerf, J. J., de Vos, A. F., Bresser, P., van der Zee, J. S., Pater, J. M., de Boer, A., Tanck, M., Lundell, D. L., Her-Jenh, C., Draing, C., von Aulock, S., and van der Poll, T. (2008) Lung inflammation induced by lipoteichoic acid or lipopolysaccharide in humans. *Am. J. Respir. Crit. Care Med.* **178**, 34–41
36. Pribasnig, M. A., Mrak, I., Grabner, G. F., Taschler, U., Knittelfelder, O., Scherz, B., Eichmann, T. O., Heier, C., Grumet, L., Kowaliuk, J., Romauch, M., Holler, S., Anderl, F., Wolinski, H., Lass, A., Breinbauer, R., Marsche, G., Brown, J. M., and Zimmermann, R. (2015) α/β Hydrolase Domain-containing 6 (ABHD6) degrades the late endosomal/lysosomal lipid Bis(monoacylglycerol)phosphate. *J. Biol. Chem.* **290**, 29869–29881
37. Sevastou, I., Kaffé, E., Mouratis, M. A., and Aidinis, V. (2013) Lysoglycerophospholipids in chronic inflammatory disorders: the PLA(2)/LPC and ATX/LPA axes. *Biochim. Biophys. Acta* **1831**, 42–60
38. Alhouayek, M., Masquelier, J., and Muccioli, G. G. (2018) Lysophosphatidylinositols, from cell membrane constituents to GPR55 ligands. *Trends Pharmacol. Sci.* **39**, 586–604
39. Shim, J. W., Jo, S. H., Kim, S. D., Lee, H. Y., Yun, J., and Bae, Y. S. (2009) Lysophosphatidylglycerol inhibits formyl peptide receptor-like-1-stimulated chemotactic migration and IL-1 β production from human phagocytes. *Exp. Mol. Med.* **41**, 584–591
40. Hung, N. D., Kim, M. R., and Sok, D. E. (2011) 2-Polyunsaturated acyl lysophosphatidylethanolamine attenuates inflammatory response in zymosan A-induced peritonitis in mice. *Lipids* **46**, 893–906
41. Balenga, N. A., Aflaki, E., Kargl, J., Platzer, W., Schröder, R., Blättermann, S., Kostenis, E., Brown, A. J., Heinemann, A., and Waldhoer, M. (2011) GPR55 regulates cannabinoid 2 receptor-mediated responses in human neutrophils. *Cell Res.* **21**, 1452–1469; erratum: 1641
42. Vancheri, C., Mastruzzo, C., Sortino, M. A., and Crimi, N. (2004) The lung as a privileged site for the beneficial actions of PGE₂. *Trends Immunol.* **25**, 40–46

Received for publication October 20, 2018.

Accepted for publication March 4, 2019.